ISSN 0003-701X, Applied Solar Energy, 2024, Vol. 60, No. 3, pp. 483–490. © Allerton Press, Inc., 2024.
Russian Text © The Author(s), 2024, published in Geliotekhnika, 2024, No. 3, pp. 603–613.

Plasma Vacuum-Arc Treatment Technology for the Metal Pipe Surfaces of Solar Thermal Power Plants

V. N. Arustamov[a], M. V. Kremkov[a], *, B. R. Kakhramonov[a], I. Kh. Khudaykulov[a], and Kh. B. Ashurov[a]

[a] *Arifov Institute of Ion-Plasma and Laser Technologies, Academy of Sciences of the Republic of Uzbekistan, Tashkent, 100125 Uzbekistan*

**e-mail: fund@academy.uz*

Received November 28, 2023; revised May 17, 2024; accepted May 20, 2024

Abstract—Currently, there is widespread interest in developing efficient technologies for harnessing solar energy, both in direct conversion of solar energy into electrical energy and in solar thermal power plants (STPPs). STPPs are sustainable sources of electricity due to the accumulation of heat in a heat carrier, which can be water, molten salt, or oil. The key to increasing the attractiveness of this technology lies in replacing the method of directly generating steam by heating water with solar radiation, with a receiver method using an intermediate heat transfer fluid. The technology of transferring heat obtained from solar radiation through liquid salt (a mixture of potassium nitrate and sodium nitrate, among others) imposes high demands on the pipes of this system that carry the heat transfer fluid, particularly regarding their corrosion resistance and service life. Using pipes made of ordinary steel grades with a special anti-corrosion coating applied to their inner surface can significantly reduce costs and increase the service life of the pipes, as well as the efficiency and reliability of STPPs. The study demonstrates that the method of comprehensive plasma vacuum arc treatment of the inner surface of metal pipes of various configurations, and the application of special coatings, ensures high anti-corrosion protection. For instance, applying a thin-layer coating of austenitic steel with a high chromium content (up to 28%) to samples of martensitic steel pipes resulted in 100% retention of the original sprayed material composition. Thus, the mechanical strength of the base material of the metal pipes in salt STPPs is combined with the high anti-corrosion properties of the applied material. Recommendations are provided for using plasma vacuum arc technology to ensure high operational properties of the circulating pipe systems in salt STPPs.

Keywords: salt solar thermal power plants, coating, austinite, martensite, cathode spot, plasma vacuum-arc treatment, metal pipes

DOI: 10.3103/S0003701X24602643

INTRODUCTION

Currently, there is a widespread interest in the development of efficient technologies for the use of solar energy, both in the direct conversion of solar energy into electrical energy and in solar thermal power plants (STPPs) [1–3]. Given that Uzbekistan has a large number of sunny days, the potential for using alternative solar energy is high [4, 5]. STPPs are sustainable sources of electricity due to the accumulation of heat in the heat carrier and the hybridization of energy carriers. For example, tower-type solar power plants implemented within the Solar Two project with a capacity of 10 MW are undergoing testing in Barstow, United States [6, 7]. In addition, a prototype plant with a capacity of 25 kW operates in Golden, United States [8]. Similar large-scale salt-based STPPs have been built in Morocco (160 and 580 MW) and are under construction in China (up to 6.0 GW) [9–14].

Existing tower-type STPPs use the following heat carriers and working fluids: water (steam), sodium, molten salts, air, and helium [15]. When using sodium and molten salts in the circulation scheme of an STPP, two circuits are needed, the heat carrier and the working fluid, which is most often water. For future large industrial plants, the preferred heat carriers for solar receivers are molten salts and liquid sodium, which reduce the cost per kWh by 25%. A mixture of 60% $NaNO_3$ and 40% KNO_3, thermally stable up to 600°C, is relatively inexpensive. Experiments on the corrosive activity of metal pipes have shown that this mixture interacts with most structural materials, leading to their oxidation. A promising material for the elements of the salt circuit is the Incolloy 360 alloy. For solar installations (70–1000 kW) operating at temperatures of 575–657 K and having the best performance (efficiency of 24%), it is recommended to use SYLTHERM 800, a silicone-based oil stable up to 673 K, as a heat carrier [15].

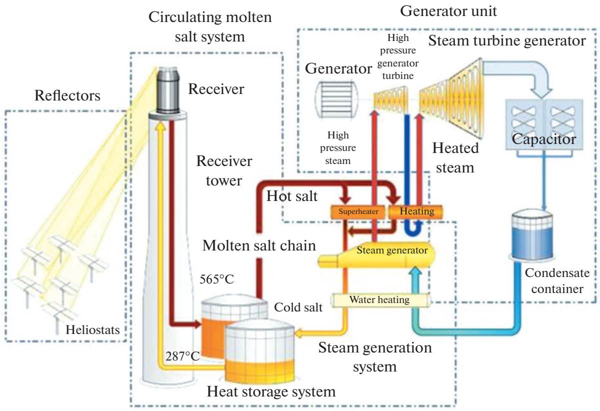

Fig. 1. Diagram of a solar thermal power plant [9].

The basis for improving the performance of this technology is the use of a scheme with an intermediate heat carrier, which is liquid salt, primarily a mixture of potassium nitrate and sodium nitrate [16]. This imposes high requirements on the corrosion resistance and lifespan of the circulation system pipes [17]. The use of ordinary steel pipes with a special anti-corrosion coating on their inner surface for these purposes will significantly reduce costs and increase the operational efficiency and reliability of salt-based STPPs. Figure 1 shows a typical scheme of a salt-based STPP [15].

From the presented scheme, it is clear that the core of the STPP technical system comprises the first and second heat carrier circulation circuits to the actuating systems, formed from high-alloy heat-resistant steel pipes. This determines a certain portion of the total cost of power plants of this type, as well as increases their lifespan, efficiency, reliability, and cost effectiveness. A unique feature is the use of liquid sodium as a heat carrier, which removes heat from the radiation receiver. The back wall of the receiver is a semi-cylinder with austenitic steel tubes with an active area of 17 m^2 through which liquid sodium circulates.

The operating principle of an STPP is as follows. Heliostats [18–21] reflect incoming sunlight onto an integrated receiver-evaporator with molten salt, which has an insulated partition separating the hot and cold parts of the molten salt. The metal pipes of the evaporator, as well as the outlet pipe, are connected to the steam drum and the water drum. The solar flux formed by the helioconcentrator heats the molten salt, which then rises through a hot curved structure (leg) and transfers its stored heat to the system of parallel evaporator pipes located in the cold part (leg) of the molten salt loop. The superheated steam is then supplied to the turbine blades. The cooled molten salt returns to the receiver through a drain channel [22, 23]. The advantage of this technology using molten salt in STPPs is that it allows power to be supplied on demand, not just when the sun is shining. The salt can store heat for several months, so an occasional cloudy day does not affect the availability of electricity. In addition, the power plant's emissions are minimal, and there are no hazardous waste byproducts [24].

The very high temperatures of the heat carrier necessitate the use of high-temperature corrosion-resistant steels. At temperatures above 1100°C, liquid fluorine salts are used as the working fluid, and a multistage turbine system is employed, allowing for efficiencies of up to 60% and significant water savings. The salt, which at these temperatures looks and flows almost like water, passes through a heat exchanger to generate steam for operating a standard turbogenerator [25].

The presence of a significant number of metal structures in STPPs, operating in the mode of thermal and chemical action on the inner surface of tubular and other internal strip elements of the transport storage exchange system, imposes high requirements on the products and materials of metal structures, which are made of high-alloy steels.

At the same time, cleaning the surface [26] of the metal pipes used in salt STPPs from scale, oxide film, rust, and other contaminants, as well as improving the surface properties of these metal pipes, increasing their microhardness, adhesion, and corrosion resistance, is a relevant task in modern solar energy. Traditionally used methods for this purpose, such as acid-alkaline etching, sandblasting, and shot blasting, are not environmentally safe and do not meet modern requirements. Moreover, the treated surface, when exposed to aggressive environments (high-temperature salt), is subject to corrosion again. Environmentally friendly and economically advantageous comprehensive technologies for processing and cleaning the surfaces of metal products of various configurations and shapes from oxides and contaminants, with the application of protective anti-corrosion coatings, can most effectively be implemented using vacuum ion-plasma technologies.

The supply of salt from the receiver and back to it from the storage tank is carried out through a system of heat-resistant steel pipes capable of withstanding high temperatures (over 1000°C). Additionally, pipes of a certain length, diameter, and wall thickness are subjected to active exposure to the heated salt solution, leading to oxidation of the inner surface of these pipes, their wear, and a reduction in their service life. Therefore, it is necessary to apply antioxidant coatings to the inner surface of the pipes. This is most appropriately and economically feasible to achieve by ion-plasma application, with high adhesive resistance, so that the coating does not peel off from the main material of the pipe during high-temperature heating and allows for low-temperature welding of individual pipe sections and bending them without compromising the integrity of the applied coating. Thus, the vacuum process of plasma vacuum-arc deposition of such coatings must satisfy the assembly and operational processes of the molten salt circulation system pipes and their supply to the steam generation system of the STPP.

MATERIALS, METHODS, AND OBJECTIVES OF THE STUDY

Active research conducted for many years at the Arifov Institute of Ion-Plasma and Laser Technologies (formerly the Institute of Electronics), Academy of Sciences of the Republic of Uzbekistan in the field of vacuum arc discharge physics and the targeted use of the results from these fundamental studies in the development of ion-plasma surface treatment technologies based on vacuum arc discharge have predetermined the development of methods for cleaning the surfaces of ferrous and non-ferrous metals from various contaminants. This has allowed for the replacement of chemical and other aggressive methods of surface treatment of metal products, as well as plasma torches for applying multifunctional protective coatings and creating multilayer materials with specified properties.

This technology is based on the interaction of vacuum arc discharge plasma with the surface of the treated metal product. The specific effect of the vacuum arc discharge on the material surface is due to the high energy concentration in the rapidly moving cathode spot, the short-term local heating of the surface, and the subsequent rapid cooling, which helps to increase the mechanical strength of metal parts and products, as well as improve their anti-corrosion and other properties.

The cathode micro-spots (CMSs) created during vacuum arc discharge are characterized by high current density (10^5–10^6 A/cm^2) [27], released energy of approximately 10^3–10^7 W/m, and temperature (~3–4 × 10^3 K), with a cathode spot size of 10^{-4} cm^2, chaotic movement over the surface of the metal product at speeds of up to several hundred meters per second, depending on the condition of its surface. This allows the use of vacuum arc discharge as a source of ion-plasma flow of cathode material for subsequent deposition on products, surface cleaning of the product (cathode), thermal treatment, quenching, mini-melting processes, forming various subsurface compositions.

Objective—To assess the feasibility of applying the developed method of comprehensive plasma vacuum arc treatment to the inner surface of metal pipes of various configurations and the application of special coatings to ensure high anti-corrosion protection of the surface, which will significantly extend the service life of steel pipes used in STPPs and improve the efficiency and reliability of the system with circulating molten salts in STPPs. Based on the research conducted, recommendations will be provided for the use of plasma vacuum arc technology to ensure the reliability and high operational properties of the circulation pipe system in STPPs.

RESULTS AND DISCUSSION

Figure 2 shows a photograph of the frontal section of metal surfaces (X18H10T steel) of a cleaned hot-rolled strip with a width of 50 mm (Fig. 2a) and a sample pipe made from this strip material (Fig. 2b). As seen in Fig. 2, the surface exposed to arc discharge, i.e., the cleaned surface, is completely free of scale. On the front of the cleaned metal pipe, traces of cathode spots spreading towards the uncleaned area are visible. Cathode spots on their path completely remove contaminants. Due to the chaotic movement of the cathode spots and the selectivity of their burning on areas with foreign coatings compared to the base material, the entire surface exposed to the vacuum arc plasma is cleaned of scale.

The samples subjected to cleaning included hot-rolled strips from II KP steel, hot-rolled strips from X18H10T steel, cold-rolled strips of 30-grade steel, and wire rod 6–8 mm from 65G, 12X18H10T, and P6M5 steel.

Samples of pipes made from XCrNiMo16-5-1 martensitic steel, after plasma cleaning their inner surface, were coated with austenitic steel with a high chromium content (up to 28%). The obtained coatings have a 100% replication of the original sprayed material composition. Optimal arc discharge currents for cleaning the inner surface of the pipe samples are 180–190 A for 30-grade steel and 195–200 A for 12X18H10T steel.

The results of the energy costs for the cleaning process of 12X18H10T steel from scale thickness on the treated surface are shown in Fig. 3.

It can be seen from Fig. 3 that the energy costs increase with the thickness of the scale on the treated surface.

STUDY OF THE ROUGHNESS OF THE TREATED SURFACE

When the arc discharge impacts the surface, local heating of the material to high temperatures occurs in the spot area. Material erosion happens in the form of explosive evaporation, resulting in craters on the surface, with solidified waves of splashed molten material on the edges. Figure 3 shows fragments of processed samples. It can be seen that craters and metal emissions caused by its evaporation and explosive processes are clearly visible on the cleaned surface.

Figures 4a and 4b show photographs of the craters formed on the surface by cathode spots at 10^{-4} Torr pressure and the sample surface (×600) at 10^{-1} Torr pressure, from which it is evident that there are no craters on the surface. Thus, increasing the pressure in the vacuum chamber leads to the removal of material from the surface without significantly altering its surface topography. As the pressure decreases in the vacuum chamber, the surface roughness increases. Increasing the volume pressure enhances discharge

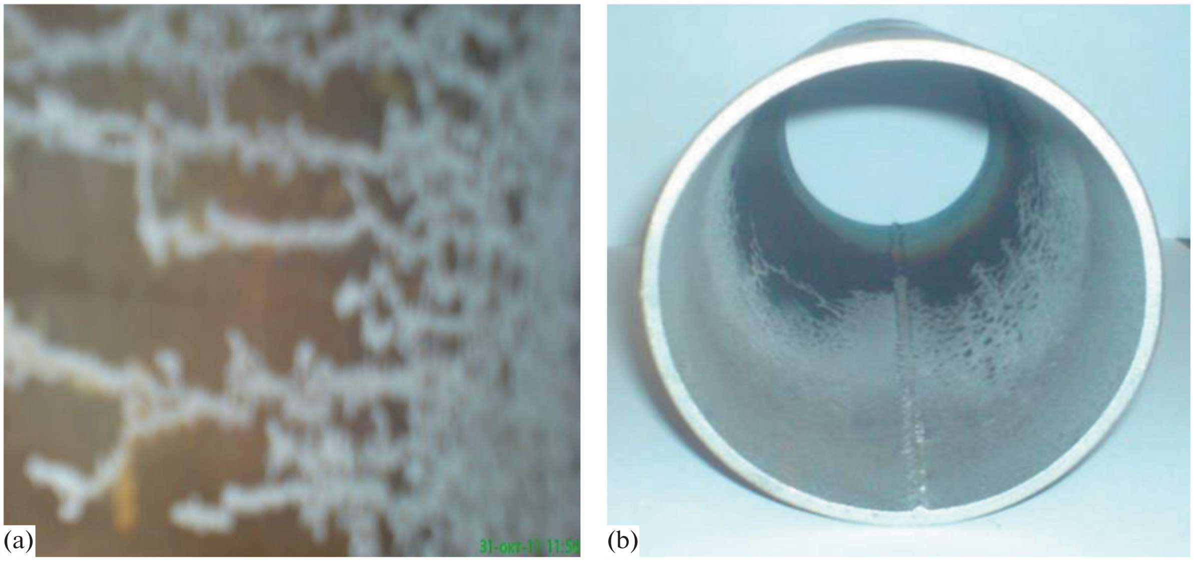

Fig. 2. View of the inner surface of a metal pipe treated with a plasma arc vacuum discharge: (a) fragment of the treated pipe surface; (b) sample of the pipe with the treated inner surface.

stability and reduces the minimum level of material vapor entry into the arc gap. Increasing the pressure in the vacuum chamber changes the characteristics of the cathode spot trace on the part, making it broader, increasing diffusion glow, and decreasing its movement speed.

The technological process was refined on 08KP strip steel. Cleaning was performed at a discharge current of 180–200 A, corresponding to a mode where 100% removal of contaminants from the surface was observed. Visual monitoring of the arc behavior was conducted with pressure changes in the volume from 10^{-1} to 10^{-2} Pa. It was noted that at 10^{-1} Pa, complete cleaning occurred, with both chaotic movement of cathode spots, represented as branched lines, and spark glows over the entire area subjected to the arc's action. At this pressure, the arc burning was accompanied by an aura glow around the discharge column. Lowering the pressure was accompanied by a decrease in the aura's glow, which disappeared at around 5–1 × 10^{-1} Pa.

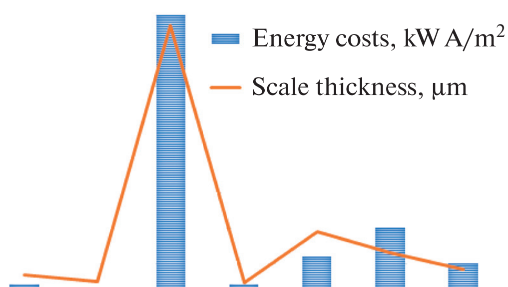

	1	2	3	4	5	6	7
Energy costs	2	1	40	2	6	10	5
Scale thickness	0.67	0.5	7.7	0.47	1.9	1.3	0.85

Fig. 3. Energy consumption for cleaning steel with an arc discharge in a vacuum as a function of scale (deposit) thickness.

Vacuum-arc treatment modes of the inner surface of P6M5 pipe were studied to determine the possibility of regulating the surface roughness class. The surface roughness of the initial and treated surface was measured using a model 201 profilograph-profiler by reading surface microroughness indications on the instrument's scale. Roughness measurement of the initial pipe sample surface (profilometry) was conducted along the generatrix over a base length of 0.8 mm. Measurements showed that the roughness ranged from 0.6 to 0.95 µm, corresponding to class 7 surface roughness according to GOST (State Standard) 2789–73. It was found that the surface roughness cleaned by arc discharge in a vacuum significantly depends on the cleaning modes. This dependence of the roughness class on the specific charge is shown in Fig. 5.

At low energy densities (specific charge 8–10 C/cm^2), the surface roughness of metal products remains almost unchanged and falls within the initial roughness class, and in some cases, the roughness class may increase. At flow densities of 10–15 C/cm^2, the roughness increases, and the roughness class drops to class 6 or lower. At flow densities above 18 C/cm^2 (studies were conducted up to densities of 26 C/cm^2), the roughness class drops to class 6 or lower. Thus, by adjusting the cleaning mode of a steel sample, it is possible to achieve the desired surface roughness after cleaning.

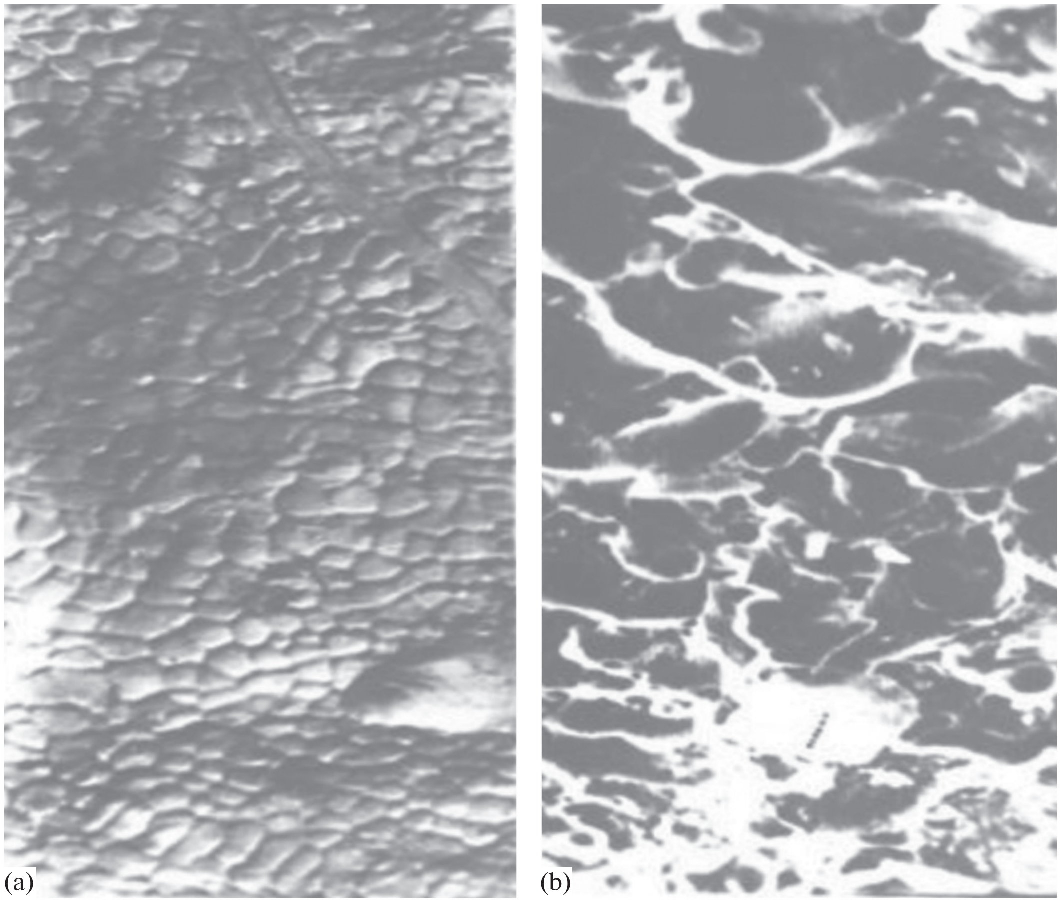

Fig. 4. Photograph of the surface (×600) after exposure to the vacuum arc discharge: (a) at a pressure of 10^{-1} Pa; (b) at a pressure of 10^{-2} Pa.

THE EFFECT OF ARC DISCHARGE CURRENT ON CLEANING PARAMETERS

The removal of material from the surface of a metal product (pipe) is carried out by cathode spots of the discharge the number of which increases with the growth of the arc current. The area affected by the cathode spots can be determined according to [28] as:

$$S = nvd, \quad (1)$$

where n is the number of cathode spots, v is their velocity, and d is the diameter of the cathode spot.

According to literature data, the current per spot is approximately 10–30 A [29]. The track cleaned by a cathode spot at a pressure of 8×10^{-2} Pa is 0.5–1.0 mm wide. The velocity of cathode spots is 10^2–10^3 cm/s. Substituting these values, we obtain the cleaning area equal to 100–200 cm^2/s. This is the upper limit of productivity since in reality, cathode spots pass multiple times over the same area, and their velocity is not constant, depending on the thickness and type of scale and contaminants.

The data on the cleaning of U-60 steel surface in percentage as a function of the arc current are summarized in Table 1. A higher current value is needed to clean strips with a greater density and thickness of the oxide film. As seen from Table 1, complete cleaning occurs at an arc current of 200–320 A, with visible individual cathode spot traces that do not increase the initial

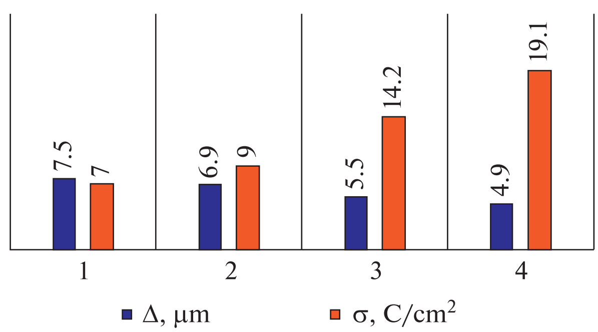

Fig. 5. Dependence of surface roughness class on the treatment mode of an 08KP strip.

Table 1. Cleaning of the surface of U-60 steel depending on the magnitude of the electric vacuum arc current

Current, A	Cleaning percentage of surface 3.2 mm wide
80	50–60
100	70–80
120	90–95
135	95–96
170	98–99
190	99–100
200–220	100

surface roughness. Moreover, in some cases, the scale was not removed from cavities on the strip surface.

Figure 6 presents the dependence of the cleaning percentage of a tubular product's surface on the arc discharge current. The graph shows that at an arc current of 60 A, the cleaning percentage of the spherical and flat surfaces (a) significantly differs from that of the tooth recess surface (b). Only at a current of 180–200 A does the cleaning percentage of flat, spherical, and tooth recess surfaces reach 100%, although spherical and flat surfaces are completely cleaned of scale at a current of 125 A.

Isolated traces of erosion, which do not increase the initial surface roughness, appear only at an arc discharge current of 180–200 A. Typically, the characteristic size of the micro-irregularities from cathode spot traces on the cleaned surface does not exceed 2.9 μm.

Therefore, double treatment of the product (if it is not fully cleaned during the first pass), usually does not lead to complete surface cleaning. In contrast, a single processing pass with a cumulative current completely removes scale from the surface. Multiple passes lead to metal removal and hardening of the sample. The rate of surface layer removal for 45 steel is 1.8 g/min at an arc discharge current of 190–220 A.

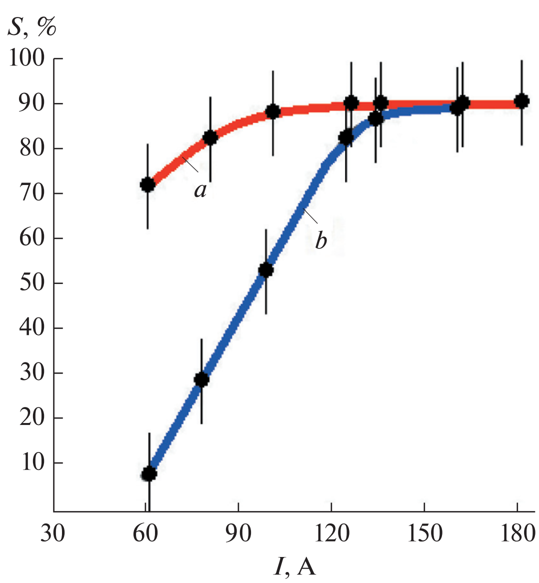

Fig. 6. Dependence of the cleaning area percentage of various surfaces of a tubular product on the arc discharge current.

The optimal final technological mode of plasma vacuum arc surface treatment involves applying a micron-thick anti-corrosion coating to the inner surface of a metal pipe up to 1.5–2.0 m in size, with a diameter of 15–35 cm and wall thickness of 3–5 mm. This mode can be recommended for the processing technology of steel pipes in the circulation system of a salt-based STPP.

The technology and processing mode we developed for the surface treatment of metal pipes of various configurations by exposure to a stable plasma vacuum arc discharge increase the strength, wear resistance, and corrosion resistance of the treated steel surface. It is characterized by high productivity and ecological cleanliness. Based on the results, we believe that this technology can be recommended for treating the inner surface of metal pipe systems in salt STPPs, as well as evaporative heat exchange and steam superheating panels made of carbon steel (A-106GRB), pipelines made of austenitic steel, and other metal pipe structures used in thermal solar energy to enhance their anti-corrosion properties, operational reliability, and service life.

CONCLUSIONS

The technology of transferring heat obtained from solar radiation through liquid salt (a mixture of potassium nitrate and sodium nitrate, etc.) imposes high requirements on the metal pipes of the circulation system in salt-based STPPs: their corrosion resistance and service life. It has been shown that the method of comprehensive vacuum arc treatment of the inner surface of metal tubular products of various configurations, including steel pipes, and applying special coatings to their inner surface, ensures their high anti-corrosion protection.

Treatment with an arc discharge increases the microhardness of the near-surface layer of the metal pipe to a depth of 2–15 μm, depending on the discharge current. The time required for metal removal by vacuum arc discharge for 45 steel is 1.82 min at an arc discharge current of 190–220 A. The microhardness of the surface layer of the metal pipe after plasma vacuum arc treatment increases by 1.5–1.7 times, and corrosion resistance increases by 10 or more times compared to the untreated surface.

X-ray analysis and secondary ion mass spectrometry methods have shown that the distribution of alloying impurities in the modified layer of the steel pipe leads to the enrichment of the surface layer with alloying elements (Mn, Cr, N) and chemically bonded carbon, which also contributes to the strengthening of the tubular product surface.

The technology we developed for treating the surface of tubular products (metal pipes) of various configurations by exposure to a stable vacuum arc discharge increases the strength, wear resistance, and corrosion resistance of the treated steel surface and is characterized by high productivity and ecological cleanliness. We believe that this technology can be recommended for treating the inner surface of elements in salt-based STPPs, as well as evaporative heat exchange, steam superheating panels made of carbon steel (A-106GRB), pipelines made of austenitic steel, and other metal pipe structures used in thermal solar energy to enhance their anti-corrosion properties, operational reliability, and service life.

ACKNOWLEDGMENTS

The authors are grateful to the staff of the Laboratory of Ion Plasma Technologies, Arifov Institute of Ion Plasma and Laser Technologies, Academy of Sciences of the Republic of Uzbekistan for discussing the results of the article.

FUNDING

This work was supported by ongoing institutional funding. No additional grants to carry out or direct thisparticular research were obtained.

CONFLICT OF INTEREST

The authors of this work declare that they have no conflicts of interest.

REFERENCES

1. Pachauri Shonali, et al., Access to modern energy: Assessment and outlook for developing and emerging regions, 2012.
2. Avezov, R.R., Avezova, N.R., and Rakhimov, E.Y., The thermal model of a flat-plate solar water-heating collector, *Al'tern. Energ. Ekol.,* 2016, nos. 23–24, pp. 12–20. https://doi.org/10.15518/isjaee.2016.23-24.012-020
3. Avezova, N.R., Khaitmukhamedov, A.E., Usmanov, A.Y., and Boliyev, B.B., Solar thermal power plants in the world: The experience of development and operation, *Appl. Sol. Energy,* 2017, vol. 53, no. 1, pp. 72–77. https://doi.org/10.3103/S0003701X17010030
4. Anarbaev, A.I., Zakhidov, R.A., Orlova, N.I., and Tajhiev, U.A., Division of Uzbekistan territory into districts based on complex of meteorological factors affecting the operational efficiency of solar hot water supply systems, *Appl. Sol. Energy,* 2008, vol. 44, no. 2, pp. 113–122. https://doi.org/10.3103/S0003701X08020114
5. Avezova, N.R., Rakhimov, E.Yu., and Izzatillaev, J.O., Resource indicators used for solar photovoltaic plants in Uzbekistan part 1, *Appl. Sol. Energy,* 2018, vol. 54, pp. 273–278. https://doi.org/10.3103/S0003701X18040023
6. Gilbert, R. and Pacheco, J.E., *Overview of Recent Results of the Solar Two Test and Evaluations Program,* Albuquerque, NM: Sandia Natl. Lab., 1999.
7. Valenti, M., Storing solar energy in salt, *Mech. Eng.,* 1995, vol. 1, no. 117(6).
8. Zhang, H.L., et al., Concentrated solar power plants: Review and design methodology, *Renewable Sustainable Energy Rev.,* 2013, vol. 22, pp. 466–481. https://doi.org/10.1016/j.rser.2013.01.032
9. https://habr.com/ru/companies/cloud4y/articles/477004/.
10. Boulakhbar, M., et al., Towards a large-scale integration of renewable energies in Morocco, *J. Energy Storage,* 2020, vol. 32, p. 101806. https://doi.org/10.1016/j.est.2020.101806
11. Kettani, M. and Bandelier, P., Techno-economic assessment of solar energy coupling with large-scale desalination plant: The case of Morocco, *Desalination,* 2020, vol. 494, p. 114627. https://doi.org/10.1016/j.desal.2020.114627
12. Terrapon-Pfaff, J., et al., Social impacts of large-scale solar thermal power plants: Assessment results for the NOORO I power plant in Morocco, *Renew. Sustain. Energy Rev.*, 2019, vol. 113, p. 109259. https://doi.org/10.1016/j.rser.2019.109259
13. Zhuang, X., et al., LCOE analysis of tower concentrating solar power plants using different molten-salts for thermal energy storage in China, *Energies*, 2019, vol. 12, no. 7, p. 1394. https://doi.org/10.3390/en12071394
14. González-Roubaud, E., Pérez-Osorio, D., and Prieto, C., Review of commercial thermal energy storage in concentrated solar power plants: Steam vs. molten salts, *Renewable Sustainable Energy Rev.,* 2017, vol. 80, pp. 133–148. https://doi.org/10.1016/j.rser.2017.05.084
15. Thermal diagrams of solar power plants. https://www.gigavat.com/ses_optic2.php.
16. Petrova, T.I., Orlov, K.A., and Dooley, R.B., International water and steam quality standards on thermal power plants at all-volatile treatment, *Therm. Eng.,* 2016, vol. 63, pp. 896–902. https://doi.org/10.1134/S0040601516100086
17. Vijayan, P.K., Nayak, A.K., and Kumar, N., *Single-Phase, Two-Phase and Supercritical Natural Circulation Systems,* Woodhead Publishing, 2019.
18. Kribus, A., Vishnevetsky, I., Yogev, A., and Rubinov, T., Closed loop control of heliostats, *Energy,* 2004, vol. 29, nos. 5–6, pp. 905–913. https://doi.org/10.1016/S0360-5442(03)00195-6
19. Schramek, P. and Mills, D.R., Heliostats for maximum ground coverage, *Energy,* 2004, vol. 29, nos. 5–6, pp. 701–713. https://doi.org/10.1016/S0360-5442(03)00178-6
20. El-Emam, R.S. and Dincer, I., Development and assessment of a novel solar heliostat-based multigeneration system, *Int. J. Hydrogen Energy,* 2018, vol. 43, no. 5, pp. 2610–2620. https://doi.org/10.1016/j.ijhydene.2017.12.026

21. Strachan, J.W. and Houser, R.M., *Testing and Evaluation of Large-Area Heliostats for Solar Thermal Applications,* Albuquerque, NM: Sandia Natl. Lab., 1993.

22. Jin, A.J., Transformational relationship of renewable energies and the smart grid, in *Sustainable Communities Design Handbook,* Butterworth-Heinemann, 2010, pp. 217–231. https://doi.org/10.1016/B978-1-85617-804-4.00012-4

23. Ajarostaghi, S.S. and Mousavi, S.S., Solar energy conversion technologies: Principles and advancements, in *Solar Energy Advancements in Agriculture and Food Production Systems,* Academic Press, 2022, pp. 29–76. https://doi.org/10.1016/B978-0-323-89866-9.00005-5

24. Khodyrev, B.N., Krichevtsov, A.L., and Sokolyuk, A.A., Studying the processes relating to oxidation of organic substances contained in the coolant of thermal and nuclear power stations, *Therm. Eng.,* 2010, vol. 57, pp. 553–559. https://doi.org/10.1134/S0040601510070037

25. Kudinov, A.A., Ziganshina, S.K., and Gorlanov, S.P., Increasing the efficiency of a combined cycle thermal power plant by removing exhaust gases from the waste heat boiler of a gas turbine unit into the atmosphere through the exhaust tower of a cooling tower with natural air ventilation, *Ind. Energy,* 2017, pp. 33–38.

26. Arustamov, V.N., Khudaykulov, I.K., Kremkov, M.V., and Ashurov, K.B., Creation of low-ohmic copper contacts on the surface of silicon crystals for application in photocells, *Appl. Sol. Energy,* 2023, vol. 59, no. 2, pp. 95–101. https://doi.org/10.3103/S0003701X22601612

27. Arustamov, V.N., Ashurov, K.B., Kadirov, K.K., Nagaybekov, R.B., and Khudaykulov, I.K., Parameters of the cathode spot upon field emission, *J. Surf. Invest.: X-Ray, Synchrotron Neutron Tech.,* 2014, vol. 8, pp. 828–831. https://doi.org/10.1134/S1027451014020311

28. Pozharov, S.L., Mirkarimov, A.M., and Soldatov, I.V., Structure of group cathode spots on the surfaces of hot-rolled steels, *Tech. Phys.,* 1998, vol. 43, pp. 1323–1328.

29. Pavlov, V.A., On the mechanism of reverse motion of a cathode spot, *J. Appl. Mech. Tech. Phys.,* 2012, vol. 53, pp. 309–315. https://doi.org/10.1134/S0021894412030017

Translated by M. Chubarova